JAERI-M
85-141

ENHANCEMENT OF ENGINEERING ADVANTAGES IN TOKAMAK REACTOR OPERATION ASSISTED BY RF WAVES

August 1985

Satoshi NISHIO, Masayoshi SUGIHARA and Takashi OKAZAKI*

日本原子力研究所
Japan Atomic Energy Research Institute

JAERI-Mレポートは，日本原子力研究所が不定期に公刊している研究報告書です。
入手の問合わせは，日本原子力研究所技術情報部情報資料課（〒319-11 茨城県那珂郡東海村）あて，お申しこしください。なお，このほかに財団法人原子力弘済会資料センター（〒319-11 茨城県那珂郡東海村日本原子力研究所内）で複写による実費領布をおこなっております。

JAERI-M reports are issued irregularly.
Inquiries about availability of the reports should be addressed to Information Division Department of Technical Information, Japan Atomic Energy Research Institute, Tokaimura, Naka-gun, Ibaraki-ken 319-11, Japan.

編集兼発行　日本原子力研究所
印　　刷　日青工業株式会社

JAERI-M 85-141

Enhancement of Engineering Advantages in Tokamak Reactor Operation assisted by RF waves

Satoshi NISHIO, Masayoshi SUGIHARA and Takashi OKAZAKI*

Department of Large Tokamak Research
NAKA Fusion Research Establishment, JAERI

(Received August 14, 1985)

The impact of RF assisted operation scenarios on reactor design were studied. These scenarios include RF assisted, long-pulsed operation and quasi-steady state operation. Burn time, required energy and overturning force on a TF coil are the parameters examined. Two kinds of plasmas were employed; a highly elongated plasma with double null poloidal divertor and a circular plasma with mechanical (pumped) limiter. The RF assisted operation scenarios allowed the burn time to be increased from 300 seconds to 2100 seconds for an elliptical plasma and from 700 seconds to 1500 seconds for a circular plasma. These increases were for a fixed reactor size. In addition, the energy consumption for the same fusion energy preduction was reduced to 1/3 for the elliptical plasma and to 1/2 for the circular plasma. However, the total energy required for an elliptical plasma is several times greater than for a circular plasma. The burn time and energy consumption differed little between RF assisted operation and quasi-steady state operation. The cyclic stress amplitude due to overturning forces on a TF coil was reduced to negligible levels by introducing RF assisted operation scenario.

Keywords: Tokamak Reactor, RF Current Drive, Burn Time, Power Supply, TF Coil, Overturning Force, Cyclic Stress

---

* Hitachi Ltd. Hitachi Energy Research Laboratory

トカマク炉にＲＦ波を導入することによって得られる工学上の利点

日本原子力研究所那珂研究所臨界プラズマ研究部
西尾　敏・杉原　正芳・岡崎　隆司*

（1985年8月14日受理）

本論文はプラズマの低密度領域においてＲＦ電流駆動を導入したとき，トカマク炉の工学設計上どのような利点が得られるかについて述べたものである。ＲＦを用いた運転シナリオとして長時間パルス運転と準定常運転を採用し，検討項目には燃焼時間，消費エネルギーおよびトロイダル磁場コイルに作用する転倒力を選んだ。さらに対象とするプラズマ断面形状は著しく異なる平衡磁場配位を要求する2種類のタイプすなわち非円形ダイバータプラズマと円形リミタプラズマをとりあげた。

ＲＦ電流駆動を導入することによって燃焼時間については非円形ダイバータプラズマで7倍，円形リミタプラズマで約2倍の延長が確保され，消費エネルギーについては3分の1および2分の1とそれぞれ軽減される。一方転倒力については準定常運転を採用し，低密度時（非燃焼時）におけるプラズマ電流を適当に選ぶことによって従来のパルス運転にくらべて非円形ダイバータプラズマにおいてはその変動荷重を事実上なくすることができ，円形リミタプラズマにおいては約半分とすることができる。

＊　日立製作所㈱ エネルギー研究所

CONTENTS

1. Introduction 1
2. Basic Consideration and Assumption 4
2.1 Plasma and device parameters 4
2.2 Plasma equilibrium 4
2.3 Poloidal beta range for LHW operation 6
3. Impact of RF Assisted Operation on Reactor Design 7
3.1 Burn time 7
3.2 Energy consumption 10
(1) RF coil system 10
(2) RF system 11
(3) Total energy consumption 15
3.3 Overturning Force acting on a TF coil 16
4. Conclusions 19
Acknowledgements 20
References 21

目　　次

1. 序 …… 1
2. 検討のための基礎事項 …… 4
2.1 プラズマ諸元および装置諸元 …… 4
2.2 プラズマの平衡 …… 4
2.3 LHW入射のためのポロイダルベータ領域 …… 6
3. 炉の設計に及ぼすRF運転の影響 …… 7
3.1 燃焼時間 …… 7
3.2 消費エネルギー …… 10
3.3 TFコイルに作用する転倒力 …… 16
4. 結　論 …… 19

謝　辞 …… 20

参考文献 …… 21

1. Introduction

Recent experimental success in ramping up [1] and sustaining [2,3,4,5,6] plasma current by the lower hybrid range of frequencies (LHRF) suggests the possibility of steady state tokamak reactor operation. The theoretical studies [7,8] have been substantiated by these experimental results. Design studies of steady state tokamak reactors using LHW have also been carried out [9,10,11]. Almost all of the current drive experiments, however, have been restricted to low density discharges (on the order of 10^{18} m^{-3}) [2,3,4,5]. The current drive efficiency, proportional to $1/\tilde{n}_e$ ($\tilde{n}_e$: electron density) rapidly approaches zero in the high density region. The only exception is an experimental result on ALCATOR-C, where the current drive continued up to $\tilde{n}_e \sim 10^{20}$ m^{-3} [12]. One of the credible explanations of this experimental result is that the high toroidal magnetic field produced a 'window' for the current drive. It is not clear, that this sort of window can be obtained in future tokamak reactor, because $\omega_{pe}^2/\omega_{ce}^2$ in future tokamak plasmas must be considerably higher than that in ALCATOR-C. In this expression, ω_{pe} and ω_{ce} are the electron plasma frequency and electron cyclotron frequency, respectively.

If the current drive is restricted to the low density region even for future tokamaks, operating scenarios can still be developed for the mitigation of engineering difficulties. One of the possible scenarios should be an RF assisted current ramp-up, promising even under the above mentioned restriction. In this scheme the start-up phase plasma current is ramped up by LHW in the low density plasma. Assistance from transformer coils (OH coils) and/or the electron cyclotron range of frequenies (ECRF) for the current initiation and ramp-up is also possible in this phase. Throughout the burning phase, the plasma current is sustained only by volt-second from the OH coils. Long burning times or compact reactor size can result, since the volt.seconds of OH coils are little used in the start-up phase. This scenario is named Long-pulse operation and is shown as a dotted chain line in Fig. 1.

Quasi-steady state operation, a natural extertion of the Long-pulse operation, can also be proposed [13,14]. A typical scheme for

this scenario is shown as a solid line in Fig. 1. This scenario is identical to Long-pulse operation until the termination of the burn. After the burn is terminated, the plasma density is lowered (ramp-down phase). Throughout this phase, the OH coils work for sustaining the plasma current, since the plasma density is still rather high. Furthermore, the volt-seconds from equilibrium field (EF) coils is changed by a variation of beta poloidal (β_p). After the plasma density is sufficient reduced, the plasma current is driven by LHRF, while the current in the OH coils is reversed to recharge the OH coils. Both these RF assisted operation scenarios result in periodic output of fusion power. Our main concerns are in evaluating possible advantages compared to conventional pulsed operation, and the effect on reactor engineering of the completely steady-state operation. Essential differences between Long-pulsed operation and Quasi-steady operation are also evaluated. We have already listed the possible advantages expected in RF assisted operation and compare them with the characteristics of pulsed operation [15]. They are repeated in Table 1. Also shown in Table 1 are characteristics of the completely steady-state operation.

These advantages and disadvantages are closely interrelated. It will not necessarily be straightforward to establish the total advantage of the RF assisted operation compared with the conventional pulsed operation. The characteristics of the RF assisted operation must be compared with those of the conventional pulsed operation in focusing on a commercial reactor. It is presumed that most of the possible advantages in Table 1 are weakened in the commercial reactor with burn time of several hours. For example, the possible advantage of the item 2 may become negligible, since it comes from the difference in the total number of cycles. The possible advantage of item 7 also will be weakened, since a resistive volt-second becomes dominant over an inductive volt-second in the commercial reactor.

RF cossisted operation can realize the possible advantages listed in Table 1 for the next generation machines like FER (Fusion Experimental Reactor) [16,17] and INTOR [18,19]. It is the purpose of this paper to establish the preferable RF assisted operating scenario for FER. This will be done by quantitatively investigating the

mitigation of engineering difficulties of conventional pulsed operation. The evaluation criteria chosen to show significant influence on a reactor design are:

- Burn time for one pulse
- Required energy for one pulse operation

  (This required energy contains the maximum stored energy and transported energy for the poloidal field (PF) coil system, and the required RF energy for current ramp-up phase, ignition approach phase and OH coil recharging phase.)
- Over-turning force acting on a toroidal field (TF) coil

2. Basic Consideration and Assumption

2.1 Plasma and device parameters

A highly elongated, divertor-controlled plasma requires much more magnetomotive force for the equilibrium field coils in a low β_p phase than in a high β_p phase, because the equilibrium field is dominated by the shaping requirements. The interpretation seems to be as follows: A high force is required to drive the null point to the designed position for the low β_p plasma. A high β_p plasma with highly elongated shape has a tendency to become circular due to its internal pressure. Therefore, it is easier in the high β_p plasma to position the null point than in the low β_p plasma. Accordingly, the following two kinds of plasmas were employed, with the parameters shown in Table 2.

- A highly elongated plasma with double null poloidal divertor(Case A)
- A circular plasma with mechanical(pumped) limiter (Case B)

These two were chosen because they are expected to differ widely in the required magnetomotive forces to produce the equilibrium field. Comparison of the two will also show which plasma is more suitable for the RF assisted operation.

2.2 Plasma equilibrium

The PF coil system of all next generation tokamak designs, including INTOR [18,19] must satisfy two functions; contributing both to the equilibrium field and to the plasma transformer field. These are called hybrid coil sets. The PF coil locations for Case A and B are shown in Fig. 2. In this figure, coils H1 to H5 produce the equilibrium field and contribute to the plasma current transformer field. The other coils, i.e. No.4, 5, 6 coils for Case A and No. 3, 4 coils for Case B contribute only to the plasma current transformer field. It is necessary in controlling the dee-shaped plasma to control a magnetic flux (volt second), a dipole field, a quadrupole field and a hexapole field independently. Among these, the magnetic flux does not have an effect on the plasma equilibrium shape.

Therefore some arbitrariness remains in dividing the allotment of the magnetic flux between the plasma current transformer field and the equilibrium field. However, it is better to make use of the solenoid coils located near the equator plane (e.g. H1 the 'equilibrium solenoid' in Fig. 2) to economiz the total ampere-turn in producing the equilibrium field. This approach is followed by FER [16] and INTOR [18,19]. The current direction of the 'equilibrium solenoid coil' is opposite that of the plasma. Therefore, termination of the plasma burn phase is reached when the allowable still have not reached maximum field (or the allowable maximum current density) is reached in the 'equilibrium solenoid coil'. At that point the other solenoid coils maximum field. It is not necessarily effective to employ this method of providing magnetic flux to the plasma. It will be desirable for bringing out the advantages of the RF assisted operation to obtain the magnetic flux from the OH coils. It will show that this maximizes the use of the magnetic flux from the OH coils. For that purpose, it is necessary to produce the equilibrium field without using the solenoid coils. If the equilibrium field is produced by only ring coils (PF coils excluding the solenoid coil), the arbitrariness in dividing the flux allotment among the OH coils and the EF coils is lost. In Table 3, the magnetic flux allotment comparison of two cases is listed. One case is for the solenoid coil's not contributing to the equilibrium field; the other case is for the solenoid coil's producing the equilibrium field under a compromise between the total ampere-turn and the magnetic flux. The plasma parameters are common, for case A of Table 2. The plasma current transformer field supplied by only the OH coils is available in the burning phase. As shown in Table 2, this increases the magnetic flux supplied by the OH coils from 65 v.s to 105 v.s without increasing the reactor size. The increment of the total magnetomotive force for the equilibrium field is, however, only 5 MA, from 70 MA to 75 MA. Under the condition of zero current in the solenoid coil (H1 coil shown in Fig. 2), the equilibrium coil (H2 ~ H5 coils) currents and the resulting magnetic flux are shown as a function of the poloidal beta (β_p) in Fig. 3. Case B (circular plasma) requires only vertical field for the plasma equilibrium, and the required vertical

field (B_v) increases with β_p, given by $B_v \propto \frac{I_p}{R_p}\left(\ln\frac{8R_p}{a_p} + \beta_p + \frac{l_i}{2} - \frac{3}{2}\right)$ [20], where R_p, a_p and l_i are the plasma major radius, minor radius and internal inductunce, respectively. Therefore, the magnetomotive force in the EF coils increases with β_p. Case A (double null poloidal divertor with highly elongated plasma shape) requires not only a vertical (dipole) field but also a shaping field (quadrupole and hexapole fields) for plasma equilibrium. The low β_p plasma with highly elongated shape has a tendency to intensify its ellipticity, because its internal pressure in rather low. The low β_p plasma requires much more shaping field, especially the quadrupole field conponent, in order to keep the null points at the same positions as for the high β_p plasma. This increment can not be compensated by a decrease in the vertical field. Therefore, the magnetomotive force in the EF coils decrease with β_p.

The required EF coil currents for the maximum plasma current are shown in Fig. 3. These are easily calculated for a arbitrary plasma current, using the proportional relation between them.

2.3 Poloidal beta range for LHW operation

The plasma density in the RF current drive phase is lower than in the burning phase by approximate a factor of 100, and the plasma temperature does not exceed that in the burning phase. The poloidal beta range for LHW operation is then $\beta_p = 0.1$, and fortunately it is not sensitive to EF coil current in this range, shown in Fig. 3. It is assumed that $\beta_p = 0.1$ marks the point for the change from LHW current drive to OH current drive. With a very low plasma current it is possibile that the poloidal beta would be higher than 0.1, but this effect can be neglected because the EF coils current of this case are also very low.

3. The Impact of RF assisted operation on Reactor Design

3.1 Burn Time

Evaluating the burn time is equivalent to calculating the available volt-seconds for the burn phase. The formula is expressed by the following symbols.

$\Delta\psi_{ava}$: available volt-seconds for the burn phase

$\Delta\psi_H$: magnetic flux change produced by equilibrium (hybrid) coils during ignition approach (from the end of the LHW operating phase to the beginning of the burn phase), which can be calculated using Fig. 3.

$$\Delta\psi_H = \left|\psi_H(\beta_p = 0.1,\ I_p = I_p^{RF}) - \psi_H(\beta_p = \beta_p^{BURN},\ I_p = I_p^{BURN})\right|$$

$\Delta(L_pI_p)$: plasma inductive flux change during the ignition approach, which also can be calculated using Fig. 3.

$$\Delta(L_pI_p) = \left|L_p(\beta_p=0.1,\ I_p=I_p^{RF})\cdot I_p^{RF} - L_p(\beta_p=\beta_p^{BURN},\ I_p=\beta^{BURN})\cdot I_p^{BURN}\right|$$

$\Delta\psi_{OH}$: capacity of the OH coils to provide magnetic flux by a full current swing (from positive to negative). Maximum field is restricted to 8 tests. $\Delta\psi_{OH}$ is 105 v.s for case A and 100 v.s for case B.

$\Delta\psi_{res}$: flux comsumption caused by plasma resistivity during the ignition approach.
If I_p^{RF} (the RF ramp-up or sustained current) is not too low compared to the burning plasma current, it is possible to achieve additional heating in the ignition approach phase and thus economizing the flux comsumption by the plasma resistance, without violating the β_p limit.
If I_p^{RF} is not too high compared to the burning plasma current, the plasma resistive flux comsumption to be provided by the OH coils must be evaluated up to a level where the additional heating is provided. The resistance, current, temperature, density, one-turn voltage, and

energy confinement time of the plasma are indicated as R, I, T, n, V and τ_E respectively.

$$\Delta\psi_{res} = \int RI\,dt = \int RI\,\frac{dt}{\dot{I}} \propto \frac{1}{\dot{I}} \int T^{-3/2}\,I\,dt$$

$$\frac{nT}{\tau_E} \cdot V \propto RI \rightarrow T \propto I^{4/5}$$

Therefore,

$$\Delta\psi_{res} \propto \frac{1}{\dot{I}} \int (I^{4/5})^{-3/2}\,I\,dI \propto \int I^{-1/5}\,dJ$$

Here, we assume that the additional heating is provided in a range where the plasma current is higher than 75% of the burning plasma current. In the FER [16,17] design as a conventional, pulsed-operation reactor, the resistive volt-second of 28 v.s is needed to reach the burning phase. Therefore, $\Delta\psi_{res}$ is expressed as follows.

$$\Delta\psi_{res} = \begin{cases} \left.\begin{array}{ll} 28 - 8.25(I_p^{RF})^{4/5} & ---- \quad 0 \leqq I_p^{RF} \leqq \frac{3}{4} I_p \\ 3 & ---- \quad \frac{3}{4} I_p < I_p^{RF} \leqq I_p \end{array}\right\} \text{for Case A} \\ \left.\begin{array}{ll} 28 - 12.01(I_p^{RF})^{4/5} & ---- \quad 0 \leqq I_p^{RF} \leqq \frac{3}{4} I_p \\ 3 & ---- \quad \frac{3}{4} I_p < I_p^{RF} \leqq I_p \end{array}\right\} \text{for Case B} \end{cases}$$

The available volt-seconds for the burning phase, $\Delta\psi_{ava}$ can be expressed as follows.

[I] $\Delta(L_pI_p) \geq \Delta\psi_H$ (corresponding to small I_p^{RF})

i) $\Delta(L_pI_p) - \Delta\psi_H \geq \Delta\psi_{res}$

$$\Delta\psi_{ava} = \Delta\psi_{OH} - \{\Delta(L_pI_p) - \Delta\psi_H\} - \Delta\psi_{res} \quad (1)$$

ii) $\Delta\psi(L_pI_p) - \Delta\psi_H < \Delta\psi_{res}$

$$\Delta\psi_{ava} = \Delta\psi_{OH} - \{\Delta(L_pI_p) - \Delta\psi_H\} - \Delta\psi_{res} \boxed{- [\Delta\psi_{res} - \{\Delta(L_pI_p) - \Delta\psi_H\}]} \quad (2)$$

[II] $\Delta(L_pI_p) < \Delta\psi_H$ (corresponding to large I_p^{RF})

i) $\Delta\psi_H - \Delta(L_pI_p) \leq \Delta\psi_{res}$

$$\Delta\psi_{res} = \Delta\psi_{OH} - [\Delta\psi_{res} - \{\Delta\psi_H - \Delta(L_pI_p)\}] \boxed{- \{\Delta\psi_H - \Delta(L_pI_p)\} - \Delta\psi_{res}} \quad (3)$$

ii) $\Delta\psi_H - \Delta(L_pI_p) > \Delta\psi_{res}$

$$\Delta\psi_{ava} = \Delta\psi_{OH} \boxed{- \{\Delta\psi_H - \Delta(L_pI_p)\} - \Delta\psi_{res}} \quad (4)$$

where, in case of RF assisted long pulsed operation, $\boxed{\quad}$ is eliminated. Fig. 4 shows $\Delta\psi_H$, $\Delta(L_pI_p)$, $\Delta\psi_{res}$ and $\Delta\psi_{ava}$ as a function of I_p^{RF}. The plasma inductive magnetic flux supplied by the LHW current drive increases with the increase in I_p^{RF}, and the plasma resistive volt-seconds decrease. Consquently, the magnetic flux stored in the OH coils is economized and is effectively used for the burning phase. In the quasi-steady state operation both case A and B, the available volt-second will be decreased when I_p^{RF} exceeds the certain level, which is about 75% of the burning plasma current. The reason is as follow. From the end of the burn phase to the OH coils recharging phase, the EF coils have an unavaidable volt-seconds comsumption. This is not completely compensated by the reduction of the inductive magnetic $\Delta(L_pI_p)$. Thus, this shortage must be compensated by the OH coils. Consquently, at the end of the burn phase there is still some magnetic flux stored in the OH coils.

The one-turn voltage of the burning plasma of FER [16,17] calculated from the plasma temperature and dimensions to be 0.05 volt.

Therefore, the maximum burn time is 2100 seconds for case A and 1460 seconds for case B.

3.2 Energy Consumption

Tokamak PF coil operation requires large power supplies. This AC power system must provide all the power needed for the conventional pulsed operation device, with most power required at the initial stage of plasma discharge. By introducing RF power to intiate the discharge and ramp up the plasma current the power handling is simplified and is no longer a critical problem. This simplifies the power handling without using the resistive volt-seconds in the plasma current ramp-up phase. An essential issue is not the power handling but the energy transport or the energy consumption. Among the many systems which require power supplies, only the PF coil system and the RF system are discussed in this paper. The cryogenic system, vacuum pumping system, cooling system, etc seen to be independent of I_p^{RF}.

(1) PF coil system

The work load on the power supply system is only the energy transport between the superconducting PF coil system and the power supply. In general, the transported energy from a state I to II is not expressed by the difference of the stored energy in the PF coil system between the state I and II, but is expressed by the sum of the absolute energy transport into/out of each PF coil as follows.

$$\Delta E = \sum_i \int_I^{II} | V_i \, I_i | \, dt \tag{5}$$

where, V_i and I_i are the terminal voltage and current of the i-th coil. Formula (5) can be rewritten by using $V_i = \sum_i M_{ij} \frac{dI_j}{dt}$, provided the PF coil is super conducting, where M_{ij} is a mutual inductance between i-th and j-th coils.

$$\Delta E = \sum_i \int_I^{II} \left| I_i \sum_j M_{ij} \, dI_j \right| \tag{6}$$

Formula (6) shows that even without a difference of the stored energy

in the PF coil system in state I and II, the energy transport leads to $\Delta E=0$ and consquently the power supply system does work. The states selected for evaluating the energy transport are at the beginning and end of each phase shown in Fig. 1.

The energy transport (E_t) for one cycle and the stored energy (E_s) are shown as a function of I_p^{RF} in Fig. 5. The energy transport of Case A rapidly increases at the region of $I_p^{RF} \gtrsim 4$ MA where the stored energy is larger in the low β_p phase (state ① or ④ in Fig. 5) than in the burning phase. Here, the transported energy in the ramp-up phase is neglected for quasi-steady operation.

The low I_p^{RF} leads to small energy transport, but low I_p^{RF} also means a short burn time. Therefore, it is useful to normalize the energy transport by the identical burn time. Figure 6 shows that the energy transport is normalized to the maximum available volt-seconds, 105 v.s for case A and 100 v.s for case B. It may also be necessary for a fair comparison between case A and case B to multiply case B in Fig. 6 by 2.26 ($= \frac{2100 \text{ second}}{1460 \text{ second}} \times \frac{440 \text{ MW}}{280 \text{ MW}}$). Even if this correction is considered, the elliptic plasma requires much more energy transport than the circular plasma. Little difference is seen between the RF assisted long pulse operation and the quasi-steady state operation.

(2) RF system

Current ramp-up, current drive and the additional heating to ignition can be carried out by RF system.

First, in ramping up and sustaining the plasma current by LHW, the main concern is how the plasma parameters (current, poloidal beta, temperature and density) must be varied. We have already reported the physics consideration for the current ramp-up and the current maintenance by RF [15,21]. Only an outline is included here. The following simplified point-model, power balance equations for the avarage electron and ion temperature $\bar{T}_e$ and $\bar{T}_i$ are used.

$$G_e P_\alpha + P_{rf} + P_J + P_{\chi e} - P_{sy} - P_{br} - P_{ei} - P_{imp} = 0 \quad , \tag{7}$$

$$(1 - G_e)P_\alpha + P_{ei} - P_{\chi i} = 0. \tag{8}$$

Here G_e is the fraction of α-particle energy transfered to the electrons, and we use the following simple expression [22], $G_e = (1 - \bar{T}_e/1.5\times10^5)^2$, and P_α, P_{rf}, P_J, $P_{\chi e}$, $P_{\chi i}$, P_{sy}, P_{br}, P_{ei} and P_{imp} are α-particle heating, deposited power by current drive, joule heating by OH current, electron and ion transport energy loss, synchrotron radiation loss, bremsstrahlung radiation loss, electrion ion energy relaxation loss and radiation loss by impurities per unit volume, respectively.

When the Rf intensity is sufficiently large, the saturated driven current density $j_{rf}(r)$ and deposited power per unit volume $P_{rf}(r)$ are given as [9,10]

$$j_{rf}(r) = 6.64\times10^{-9}\ \frac{n_e(r)}{\sqrt{T_e(r)}}\ \exp\left[-\frac{2.56\times10^5}{n_{z1}^2\ T_e(r)}\right]\left(\frac{1}{n_{z2}^2}-\frac{1}{n_{z1}^2}\right)(A/m^2) \qquad (9)$$

$$p_{rf}(r) = 3.79\times10^{-29}K\ \frac{n_e^2(r)}{\sqrt{T_e(r)}}\ \exp\left[-\frac{2.56\times10^5}{n_{z1}^2\ T_e(r)}\right]\ln\frac{n_{z1}}{n_{z2}}\ (W/m^3), \qquad (10)$$

where $n_e(r)$, $T_e(r)$ are electron density and temperature at the position r. All units are SI throughout the paper except for temperature (eV). n_{z1} and n_{z2} are the upper and lower refractive index of the wave in the toroidal direction. Wave spectrum takes finite value between n_{z1} and n_{z2}, and is assumed to be zero elsewhere. K is a correction factor which is obtained from the two-dimensional simuation in velocity space, and we take K = 0.392 [8]. The total driven current I_{rf} and deposited power P_{rf} are presented by using Eqs. (9) and (19) as follows.

$$I_{rf} = 2\pi\int_0^a j_{rf}(r)\ r\ dr \quad , \qquad (11)$$

$$P_{rf} = 4\pi^2R\int_0^a p_{rf}(r)\ r\ dr \quad , \qquad (12)$$

where a and R are the plasma minor and major radii, respectively.

The tokamak system can be replaced by the following equivalent circuit model in order to obtain the ramp-up time and the recharging time.

$$\frac{d}{dt}+L_p\frac{dI_p^{PFC}}{dt}+(R_p+\frac{dL_p}{dt})I_p^{PFC}+L_p\frac{dI_{rf}}{dt}+\frac{dL_p}{dt}I_{rf}+R_p^{rf}I_{rf}=0 \quad , \qquad (13)$$

where

ψ : Magnetic flux (volt-second) from the PF coil system

L_p : Plasma inductance

R_p : Plasma resistance for the current induced by PF coil system

I_p^{PFC}: Plasma current induced by PF coil system

I_{rf}: Plasma current induced by RF (considered as a constant current source)

R_p^{rf}: Plasma resistance of current circuit induced by RF

Since the current induced by RF is mainly carried by the resonant high-velocity (temperature) electrons which correspond to the tail of a Maxwellian energy disbribution, R_p^{rf} can be neglected. Furthermore as can be seen in Fig. 3, the transition of L_p can be also negligible. Therefore, the current circuit equation (13) is rewritten as follows.

$$\frac{d\psi}{dt}+L_p\frac{dI_p}{dt}+R_p(I_p-I_{rf})=0 \qquad (14)$$

where, $I_p = I_{rf} + I_p^{PFC}$ is the net plasma current. The necessary ramp-up time τ_{ramp} for raising the plasma current to I_p^{RF} is derived by the use of Eq. (14) as

$$\tau_{ramp} = -\tau \ln\left(1-\frac{I_p^{RF}}{I_{rf}}\right) \qquad (15)$$

where $\tau=\dfrac{L_p+\dfrac{\psi}{I_p^{RF}}}{R_p}$ and ψ is magnetic flux provided by EF coils when β_p=0.1 and $I_p=I_p^{RF}$, and is equal to -13.2 (v.s) $\dfrac{I_p^{RF}(MA)}{5.3\ MA}$ for case A and 18.8(v.s)$\dfrac{I_p^{RF}(MA)}{5.3MA}$ for case B respectively. This τ_{ramp} is shown in Fig. 7 as a function of I_p^{RF}. The electron density and the impurity (oxygen) content are chosen as the parameters.

The necessary recharging time for the reverse flux of one volt-second under the condition of constant plasma current, I_p^{RF}, can also

be derived by the use of Eq. (14):

$$\tau_{rech} = \frac{1}{R_p(I_{rf} - I_p^{RF})} \tag{16}$$

Fig. 8 shows the recharging time τ_{rech} for one volt-second as a function of the sustained current I_p^{RF} for case A. It is necessary for case B to make a plasma resistance correction which is derived from the differences of the plasma cross section and major radius. The recharging time for case B is 0.73 times as long as that for case A. Since the plasma equilibrium condition is kept constant during the recharging phase, there is no volt-second contribution from the EF coils.

The numerical procedure to obtain the injected RF energy $E_{RF}^{ramp} = \tau_{ramp} \cdot P_{rf}$ in the rmap-up phase and $E_{RF}^{rech} = \tau_{rech} \cdot P_{rf}$ for one volt-second in the recharging phase is as follows. First, the electron density is fixed. Second, the nonlinear equations (7) and (8) for $\bar{T}_e$ and $\bar{T}_i$ with appropriate values of the wave refractive index n_{z1} and n_{z2} are solved. Finally, by using I_{rf} consistent with the plasma power balance through P_{rf}, values for τ_{ramp}, τ_{rech}, E_{RF}^{ramp} and E_{RF}^{rech} are calculated. Fig. 9 and Fig. 10 show the E_{RF}^{ramp} and E_{RF}^{rech}, respectively as a function of I_p^{RF}. Fig. 10 is for only case A. It is necessary for case B to make the correction to the recharging time (0.73) and to the plasma volume (0.75). Consequently, the energy injection (E_{RF}^{rech}) in the recharging phase for case B is 1.04 times that for case A.

As mentioned in the introduction, recent current drive experiments with LHW have been in low density plasmas, (of order 10^{18} m^{-3}) [4,5]. According to the study of electron cyclotron heating (ECH) preionization of the plasma for a commercial reactor [11], the initial density is several times 10^{18} m^{-3}. A lower plasma density is preferable as can be seen in Fig. 7 and 8. However, if the initial plasma density is extremely low, the ECH power is not absorbed in the plasma. Though the initial plasma density can not necessarily be set by this condition, the plasma density in the ramp-up and the current drive phases is chosen as 3×10^{18} m^{-3} in this paper. The impurity (oxygen) content is taken as $f_z = 2\%$ under the assumption that it is

difficult to eliminate the impulity to a negligible level in the lower plasma density region.

Additional heating power is indispensable for the ignition approach phase. This heating power is provided by RF system and 60 MW for 5 s is the reference case for the present FER [16,17]. We also employed this 60 MW for case B. The RF energy is normarized by the maximum burn time in the same manner as for the PF coil system, and the results are shown in Fig. 11.

(3) Total energy consumption

The PF coil power converters receive AC power from the (motor generator) MG units and the utility line, and convert it to pulsed DC power needed for a normal operating cycle. Since the PF coil conductor is super conducting, the PF coil has not joule loss in its conductor, but the loss in the power converters is energy consumption. We assume that the loss in MG units is 5% (bearing loss of 1.4%, winding loss of 1.0%, core loss of 0.5%, armature copper loss of 1.0%, stray loss of 0.3%, field coil loss of 0.6 % and friction loss in flywheal of 0.2 %), the loss in the power converters is 5% and the heating loss in the feeder busses is 0.5% [23]. This gives a total loss in the PF coil system of 10.5%.

It is usually accepted that the power efficiency of the RF amplifier is 65% and the power transport effiency is about 90% [24]. The energy consumption in the RF system is then 1.71 times the RF energy injected into the plasma.

Fig. 12 shows the total energy consumption normarized to the maximum available volt-seconds, 105 v.s for case A and 100 v.s for case B, respectively. A fair comparison between case A and case B may also require multiplying case B by 2.26 ($= \frac{2100 \text{ seconds}}{1460 \text{ seconds}} \times \frac{440 \text{ MW}}{280 \text{ MW}}$).

3.3 Overturning Force acting on a TF coil

The TF coil structural design must follow a system design approach which allows it to meet not only its own requirements but also the requirements of the total device. The difficulties of supporting the super conducting TF coil of a large tokamak are mainly caused by the overturning force which result from the interaction of the TF coil current and the equilibrium field. In a pulsed operation tokamak, this force acts cyclically on TF coils. The TF coil structural design criteria include conventional (primary) stress limits in addition to limits established for the stress amplitude based on fatique life considerations. It is expected that the stress amplitude can be reduced considerably by introducing the quasi-steady state operation. Our main concern is to seek a desirable transition of plasma current which corresponds to the EF coil current.

The overturning moment about the horizontal axis (R-axis) or the vertical axis (Z-axis) is usually considered as a measure of the out-of-plane forces. The moment, which is an integrated quantity, however, is not necessarily useful for structural design. The overturning force for a highly elongated plasma is distributed along the TF coil perimeter, as shown for case A in Fig. 13. Although the large overturning force is acting on the TF coil, the overturning moment integrated around the R-axis becomes zero at $\beta_p \approx 1.5$ as shown in Fig. 14. Fig. 13 shows how the overturning force at low β_p (OH coil recharging phase or end of Rf ramp-up phase) and at high β_p (burn phase) is distributed along the TF coil perimeter for both case A and case B. Since the equilibrium field for the circular plasma (case B) is approximately uniform, the overturning force does not range from large position to large negative values. From case A in Fig. 13, one sees that the amplitude of the overturning force can be reduced by keeping the plasma current during the recharging phase at lower value than during the plasma burn.

The reduction of cyclic stress due to the overturning force on TF coil resulting from quasi-steady state operation is described as follows. The equivalent stress amplitude under the existance of a mean stress is given by the following formula and is quaranteed by

modified Goodman diagram.

$$\sigma_{eq} = \frac{\sigma_a}{1 - \frac{\sigma_{mean}}{\sigma_u}} \tag{16}$$

where, σ_a: Cyclic stress amplitude

σ_{mean}: Mean stress

σ_n: Ultimate stress

The maximum and minimum stress are denoted by σ_1 and σ_2 respectively. It is assumed that σ_1 does not exceed the ASME criteria for the primary stress, and $\sigma_1 = \frac{1}{3}\sigma_u$ is assumed. The equivalent stress amplitude for the pulsed operation (σ^P_{eq}) and the quasi-steady state operation (σ^Q_{eq}) are rewritten as follows.

$$\sigma^P_{eq} = \frac{3}{5}\sigma_1 \tag{17}$$

$$\sigma^Q_{eq} = \frac{\sigma_1 - \sigma_1}{2 - \frac{\sigma_1 + \sigma_2}{3\sigma_1}} \tag{18}$$

Unless both σ^P_{eq} and σ^Q_{eq} are so low that the fatigue life exceeds the endurance limit ($\approx 19^6$), it is useful to define $\gamma = \sigma^P_{eq}/\sigma^Q_{eq}$ as a figure of merit for the quasi-steady state operation, and γ is:

$$\gamma = \frac{1}{5} \cdot \frac{5 - \sigma_2/\sigma_1}{1 - \sigma_2/\sigma_1} \tag{19}$$

Here, the locations of maximum overturning force are chosen for evaluating the stress amplitude, and they are the point between B and C for case A and the point between C and D for case B as shown in Fig. 13. The force (f_{RF}) at this point in the recharging phase and the force (f_B) in the burn phase is related is $f_{RF}/f_B = 0.254\ I_p^{RF}$ (MA) for case A, and $f_{RF}/f_B = 0.149\ I_p^{RF}$ (MA) for case B. If the force is proportional to the stress, the fatigue figure of merit can be rewritten using f_{RF}/f_B as:

$$\gamma = \begin{cases} \frac{1}{5}\,\dfrac{5 - f_{RF}/f_B}{1 - f_{RF}/f_B} & 0 \leq f_{RF}/f_B \leq 1 \\ \frac{1}{5}\,\dfrac{5 - f_B/f_{RF}}{1 - f_B/f_{RF}} & 1 < f_{RF}/f_B \end{cases} \tag{20}$$

Fig. 15 shows γ as a function of I_p^{RF}, the sustained plasma current during the OH coil recharging phase. The features of the fatigue of merit are also shown schematically in Fig. 16. One can choose a sustained plasma current (less than the burning plasma current) which yields zero amplitude stress for a highly elongated plasma, case A.

We have examined the reduction of cyclic stress only at the most severe location. Even if the plasma current is sustained at about 4 MA in the recharging phase for case A the fatigue proble may remain at another coil location. When more detailed stress analysis locates the critical region, the stress amplitude can be reduced by applying this approach.

4. Conclusions

We employed the burn time, energy consumption, and the overturning force on a TF coil as the major items influened by introducing RF assisted operating scenarios. We showed that these items can be affected by the ramped-up plasma current for the RF assisted long pulsed operation or by the sustained plasma current for the quasi-steady state operation. There was not a major difference between the RF assisted long pulsed operation and the quasi-steady state operation for either the circular on the elliptical plasma in the burn time the operation energy consumption. The elliptical plasma requires much more magnetomotive fore for equilibrium field in the low poloidal beta phase than in high poloidal beta phase and is strongly dependent on the ramped up plasma current or the sustained plasma current. The cyclic overturning force amplitude on a TF coil for the quasi-steady start operation of an elliptical plasma can be reduced at negligible level.

The following recommendations result from this analysis: For an elliptical, divertor plasma the ramped up plasma current or the sustained plasma current should be about 75% of the value of the burning plasma current. For a circular, limiter plasma, the ramp up plasma current or the sustained plasma current should be identical with the burning plasma current. The results indicate that the cyclic stress amplitude can be made virtually zero for the noncircular plasma having the ellipticity of 1.3 by maintaining the plasma current at the same value throughout the whole phase as schematecally shown in Fig. 17. The resulting impacts of RF assisted operation scenario, compared to conventional pulsed operation, are summarized in Table 4.

Acknowledgements

The authors are grateful to Dr. K. Shinya for fruitful discussions of plasma equilibrium calculations. We are also grateful to Drs. H. Iida, N. Noboru, T. Tone for their continued encouragement throughout this work. Thanks are also due to F. W. Wiffen for assistance in preparing the manuscript.

References

[1] S. Kubo, M. Nakamura, T. Cho, S. Nakao, T. Shimozuma, et al., Phys. Rev. Lett. 50(1983) 1994.

[2] T. Yamamoto, T. Imai, M. Shimada, N. suzuki, M. Maeno et al., Phys. Rev. Lett. 45 (1989) 716.

[3] W. Hooks, S. Bernabei, D. Boyd, A. Cavallo, T.k. Chu. in: Plasma Physics and Controlled Nuclear Fusion Research, Proc. 9th Int. conf. Baltimore, 1982, IAEA-CN-41/C-5.

[4] S. tanaka, Y. Terumichi, T. Maekawa, T. Cho, M. Nakamura et al., in: Plasma Physics and Controlled Nuclear Fusion Research, Proc. 9th Int. Conf. Baltimore, 1982, IAEA-CN-41/C-1-3

[5] K. Ohkubo, S. Takamura, K. Kawahata, T. Tetsuka, K. Matsuura et al., Nuclear Fusion 22 (1982) 203.

[6] J. Stevens, S. von goeler, S. Bernabei, T.K. Chu, W. Hook et al., Phys. Rev. Lett. 50 (1983) 1944.

[7] N.J. Fisch, Phys. Rev. lett. 41 (1978) 873.

[8] C.F.F. Karney, N.J. Fisch, Phys. Fluids 22 (1979) 1817

[9] D.A. Ehst, Nuclear Fusion 19(1979) 1369.

[10] S.Y. Yuen, D. Kaplan, D.R. Cohn, Nuclear Fusion 20 (1980) 159.

[11] C.C. Baker, M.A. Abdou et al. ANL/FPP-80-1 (1980).

[12] M. Porkolab, J.J. Schuss, B. Lloyd, S. Texter et al., Phys. Rev. Lett. 53 (1984) 450.

[13] R.A. Bolton et al. Proc. 3rd ANS Topical Meeting on Technology of Controlled Nuclear Fusion, Santa Fe, NM, 1978.

[14] N.J. Fish, Proc. 4th Topical Conf. RF Plasma Heating, Austin, TX, 1981, also PPPL-1772 (1981).

[15] M. Sugihara, N. Fujisawa, T. Yamamoto, S. Nishio, T. Okazaki et al., Nuclear Engineering and Design/Fusion 1 (1984) 265-277.

[16] K. Tomabechi et al., in: Plasma Physics and Controlled Nuclear Fusion Research, Proc. 9th Int. conf. Baltimore, 1982 Vol. 1; IAEA, Vienna (1983) 399.

[17] T. Tone et al., Nuclear Technology/Fusion 4 (1983) 399.

[18] Intor Group, International Tokamak Reactor, Phase One, IAEA, Vinna (1983)

[19] Inter Group, International Tokamak Reactor, Phase Two A, IAEA,

Vienna (1983)

[20] V.S. Muhovatov and V.D. Shafranov, Nuclear Fusion 11 (1971) 605

[21] T. Okazaki, M. Sugihara, S. Nishio and N. Fujisawa, to be published in Nuclear Engineering and Design/Fusion

[22] J.F. Clarke, Nuclear Fusion 20 (1980) 563.

[23] Fusion Reactor System Laboratory (JAERI), JAERI-M 83-214 (1984) in Japanese

[24] K. Miyamoto, M. Sugihara et al., JAERI-M 82-172 (1982)

Table 1 Possible advantages for the reactor engineering by quasi-steady and completely steady-state operation scenarios. Open (closed) circle denotes the advantage (disadvantage). Size of the circule denotes the expected degree of the (dis)advantage compared with the OH long pulse operation. Hyphen represents no (dis)advantage.

Possible advantage	Major impact	Quasi-steady operation	Completely steady-state operation
1. Increase of duty cycle	• Capacity of energy reservoir	(●)	○
2. Reduction of number of thermal and mechanical stress cycle	• Thermal stress of 1st wall/divertor/blancket	-	○
	• Mechanical stress of TF coils by overturning moment	-	○
3. Reduction of variation of thermal and mechanical stress	• Heat load on 1st wall and divertor plate	○	○
	• Mechanical stress of TF coils by overturning moment	○	○
4. Reduction of magnetic energy loss of PF coils during energy transfer	• Total required energy for operation	○	○
5. Reduction of peak power in start-up phase	• Capacity of power supply	○	○
6. Reduction of AC loss in PF and TF coils in start-up/shut-down phase	• Capacity of cooling system	○	○
	• Total required energy for operation	○	○
7. RF system	• Capital cost	●	●
	• Total required energy for operation	●	●
8. Reduction of device size	• Construction cost	○	○
9. Reduction of plasma disruption	• Life of 1st wall	-	○
	• Support system for electro-magnetic force	-	○

Table 2 Plasma and device parameters

	Case A	Case B
Fusion power (MW)	440	280
Major radius (m)	5.5	5.6
Minor radius (m)	1.1	1.2*
Ellipticity	1.5 ~ 1.6	1.0
Triangularity	0.2	0
Current (MA)	5.3	3.4
Safety factor (q_ψ)	2.5	2.5
Toroidal beta (%)	4.0	2.0
Poloidal beta	3.0	2.0
Heating power in ignition approach (MW)	60	60
Limiter/Divertor	Double Null poloidal divertor	Mechanical(pumped) limiter

* Still more scrape-off layer of 10 cm is estimated in comparison with Case A.

Table 3 Magnetic flux allotment comparison between the case of solenoid coil's being released from producing equilibrium field and the case of solenoid coil's producing equilibrium field (for case A)

	Solenoid coil is used for EF	
	NO	YES
Magnetic flux from EF coil (v.s)	10	40
Magnetic flux from OH coil (v.s)	105	65
Total magnetic flux (v.s)	115	105
Ampere turn for EF coil (MAT)	75	70

Note; Maximum magnetic field in conductor is 8 tesla.

Table 4 Impact of RF assisted operation scenario in comparison with

	Elliptical divertor plasma (Case A)		Circular limiter plasma (Case B)	
	Long pulse	Quasi-steady	Long pulse	Quasi-steady
Burn time (per one pulse)	6 ~ 7 times (1500 ~ 2100 sec)	6 ~ 7 times (1500 ~ 2100 sec)	~2 times (~ 1500 sec)	~2 times (~ 1300 sec)
Energy consumption [•PF coil system •RF system (current drive and heating)] (per one pulse)	One third (~ 5 GJ)	One third (~ 5 GJ)	Half (~ 1 GJ)	Comparable (~ 2 GJ)
Overturning force	Cyclic number can be reduced by 1/6 ~ 1/7 times.	Stress amplitude is negligible small.	Cyclic number can be reduced by half.	• Cyclic number can be reduced by half. • Stress amplitude becomes half.
Recommendation	Preferable ramp-up current or sustained current is 60 ~ 70 % of burning plasma current.		Preferable ramp-up current or sustained current is the same value of burning plasma current.	

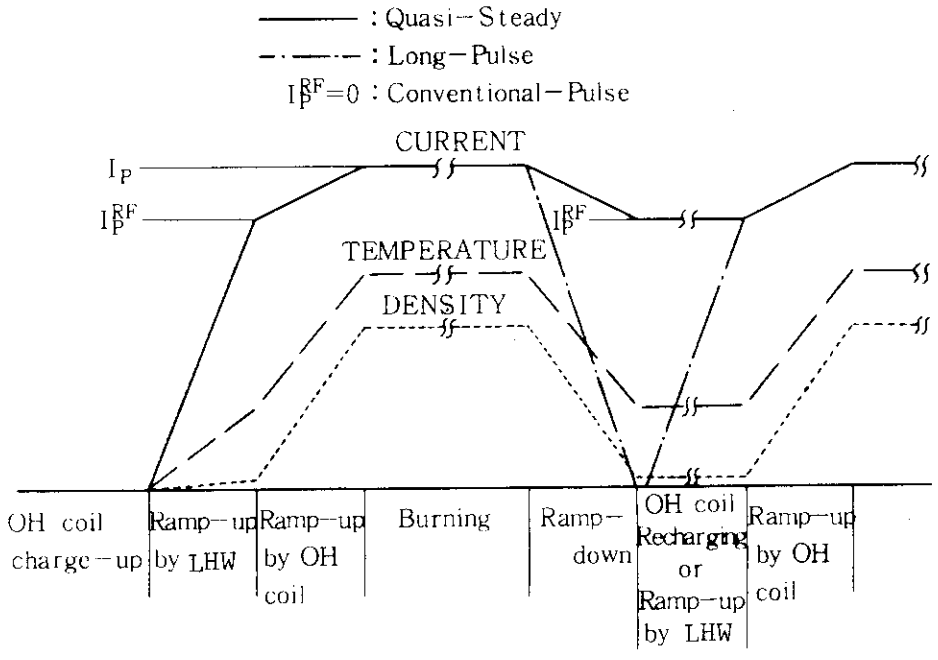

Fig. 1 Typical RF assisted operation scenarios.

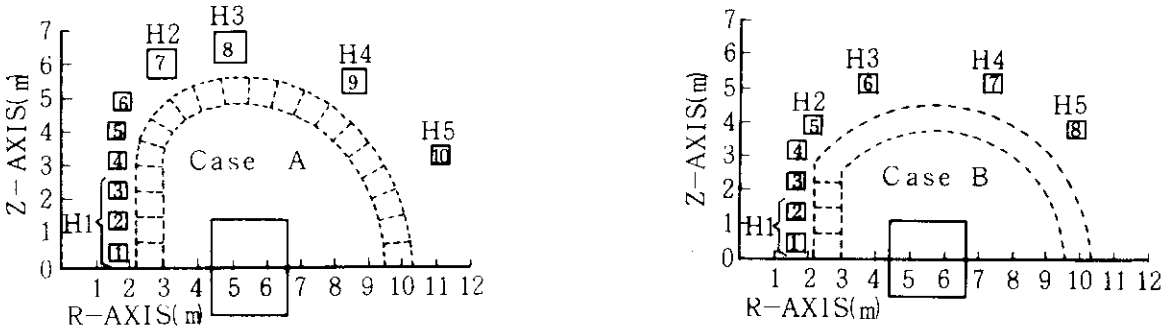

Fig. 2 Hybrid PF coil location.

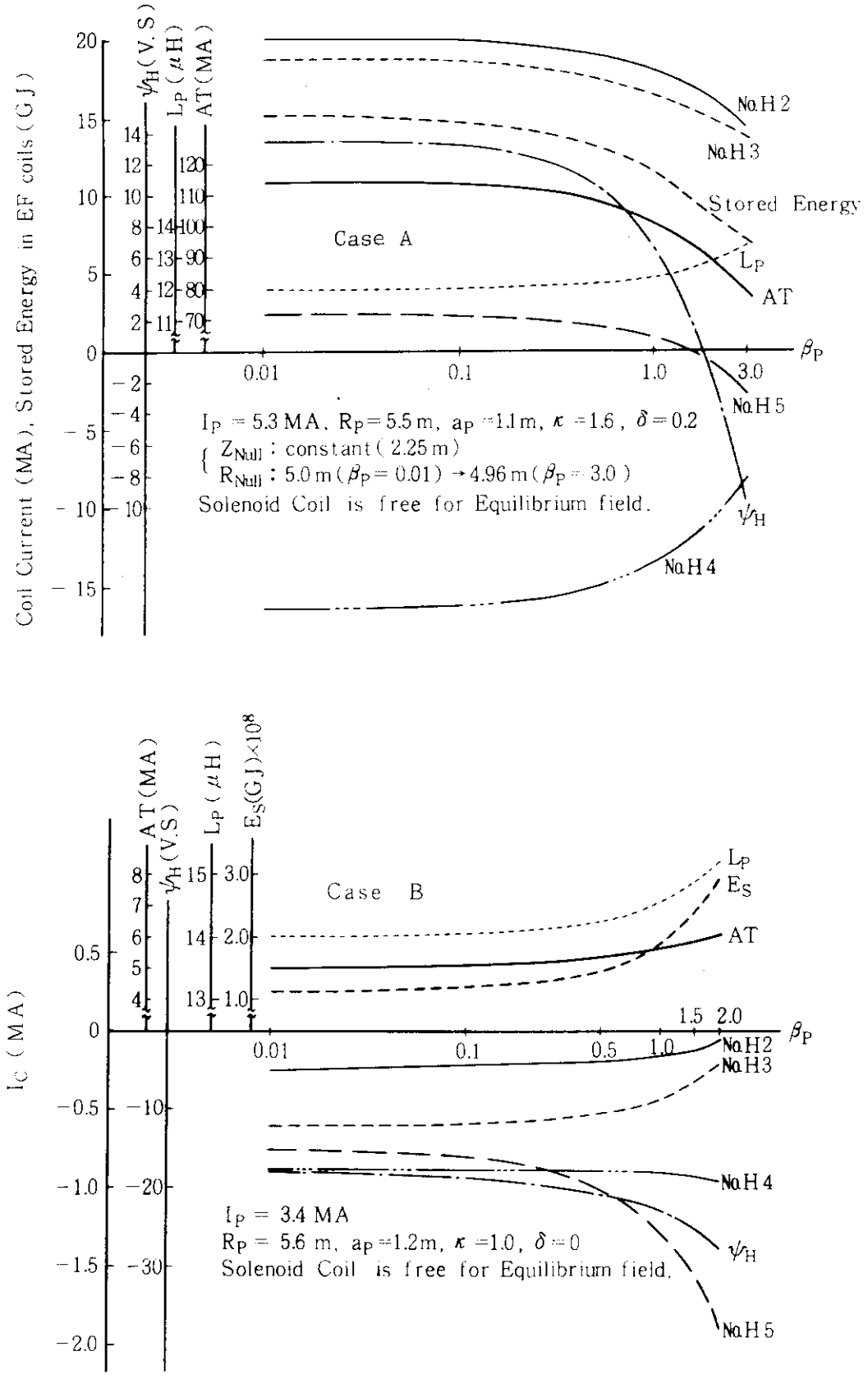

Fig. 3 Dependence of poloidal beta (β_p) on equilibrium field coil current, resultantly supplied volt-second (ψ_H) and plasma inductance (L_p) AT is total ampere-turn in equilibrium field coil.

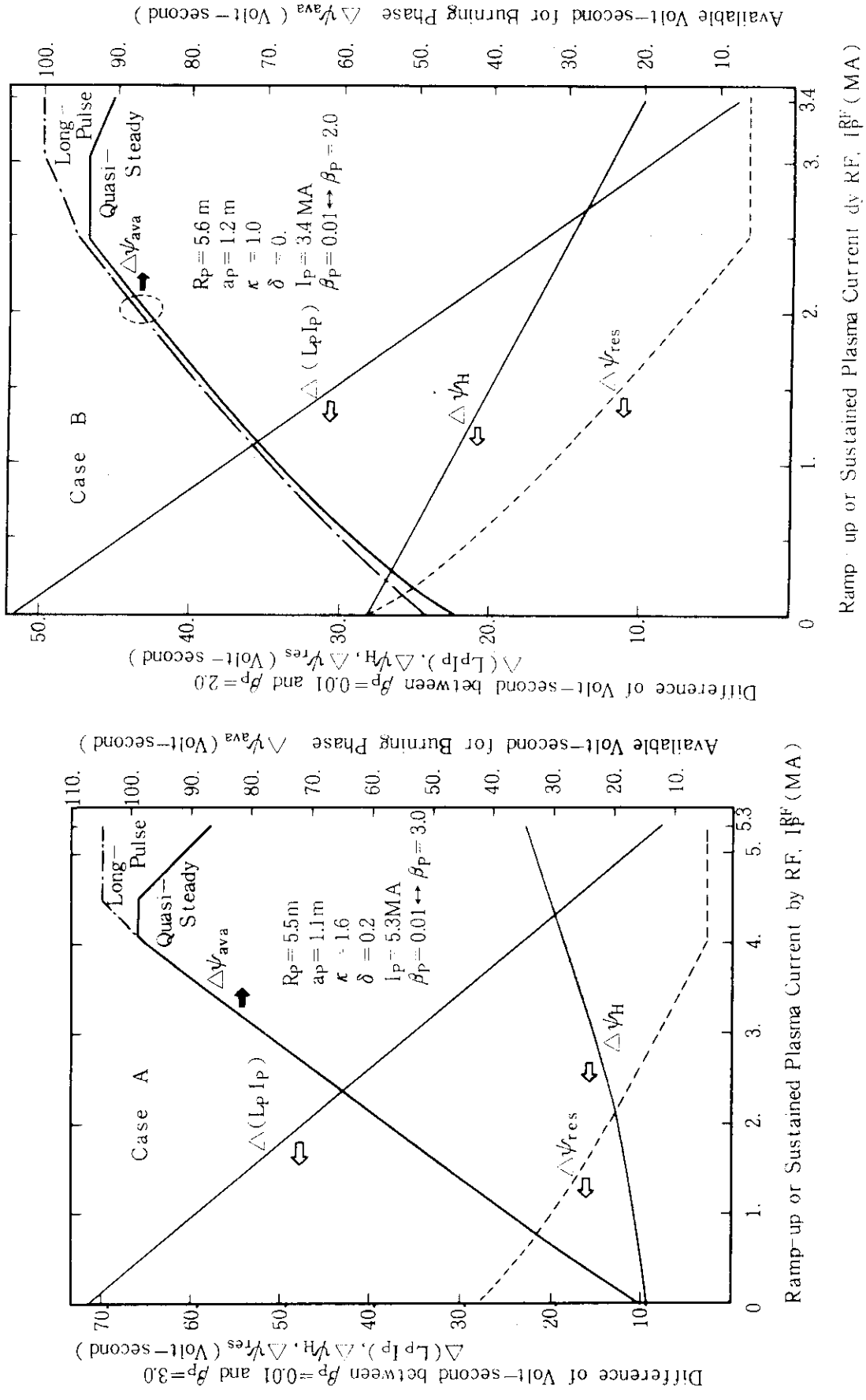

Fig. 4 Dependence of I_p^{RF} (ramped up or sustained plasma current) on available volt-second for burning phase

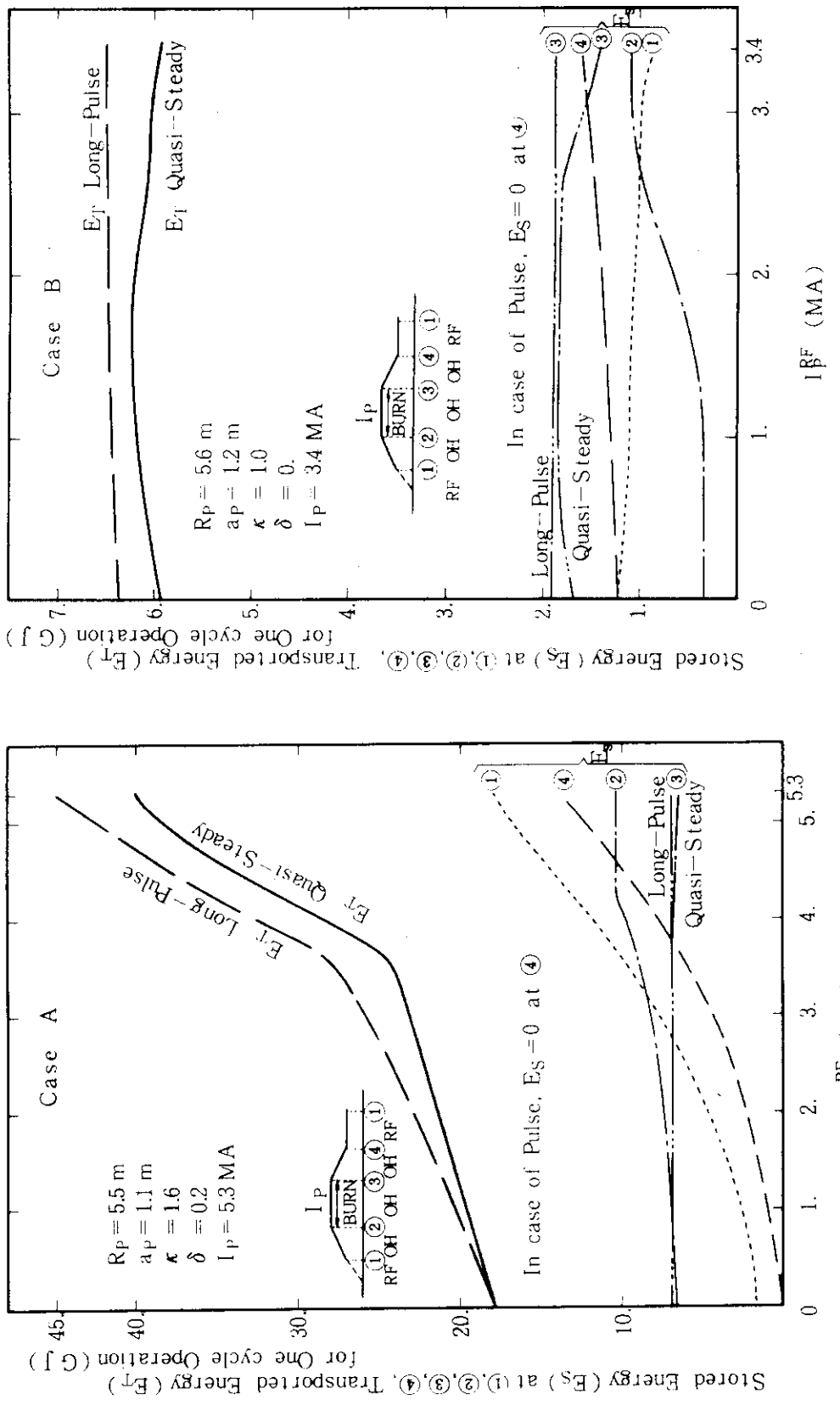

Fig. 5 Dependence of I_p^{RF} on energy transport between power supply system and PF coil system for one cycle operation, and PF coil stored energy at transition stages of each phases.

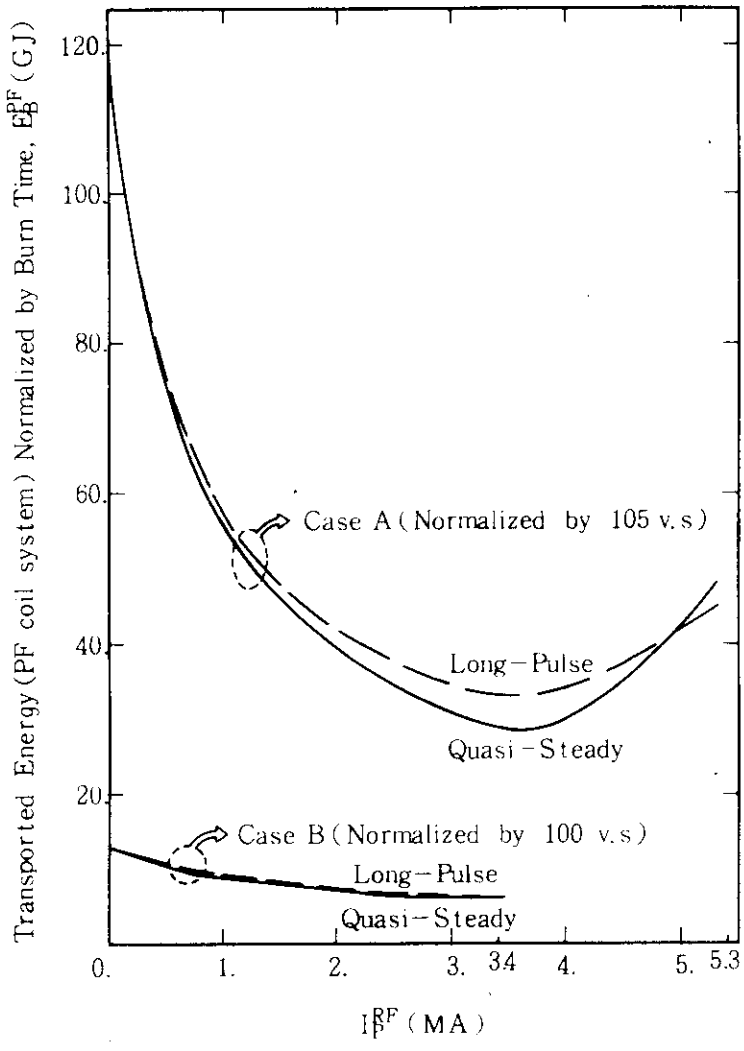

Fig. 6 Dependence of I^{RF} on normarized energy transport between power supply system and PF coil system Case A and Case B are normarized by 105 v.s and 100 v.s which are the maximum available volt-second for burn phase, respectively.

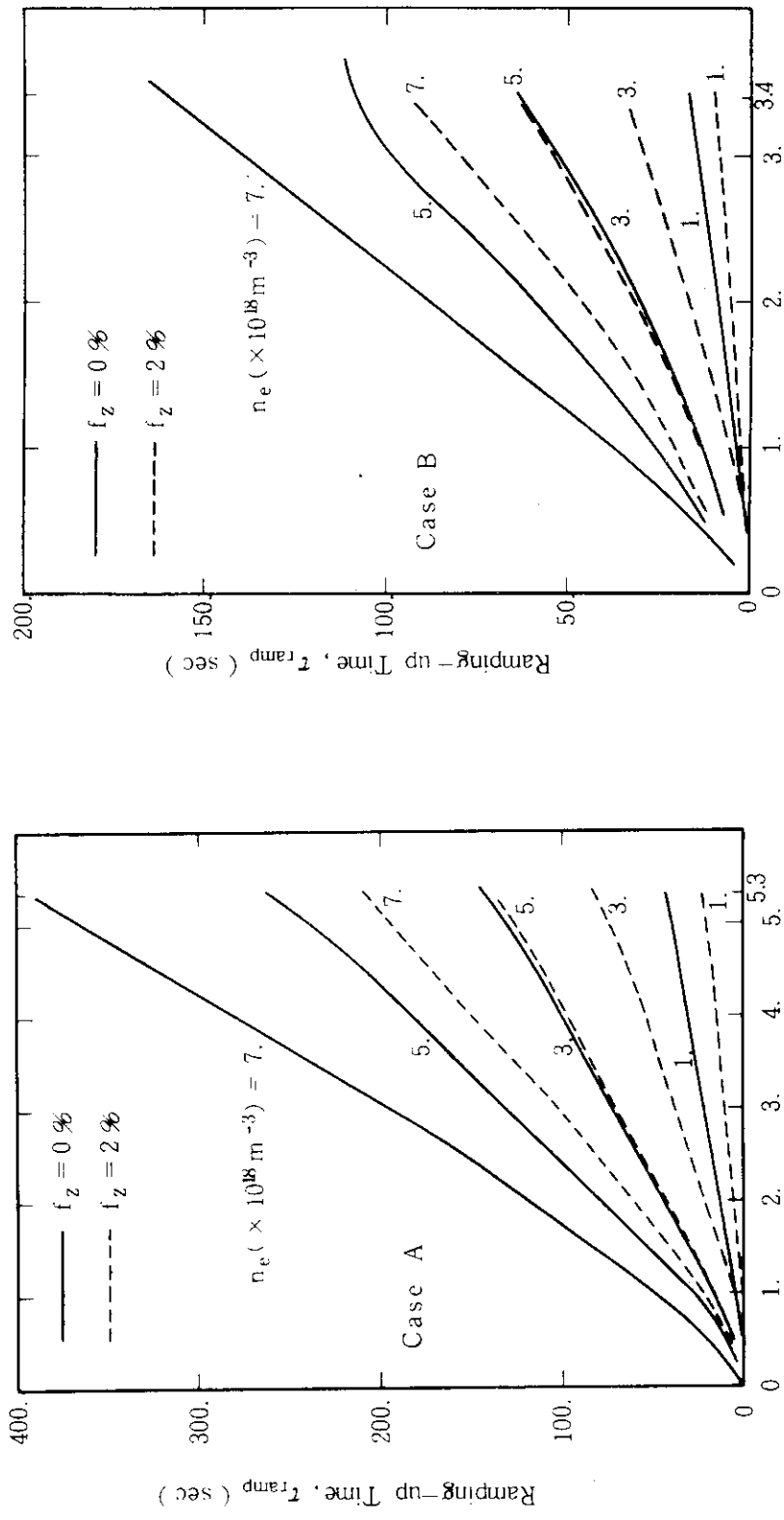

Fig. 7 Dependence of I_p^{RF} on ramp up time
(n_e and f_z are electron density and impurity (oxygen) content)

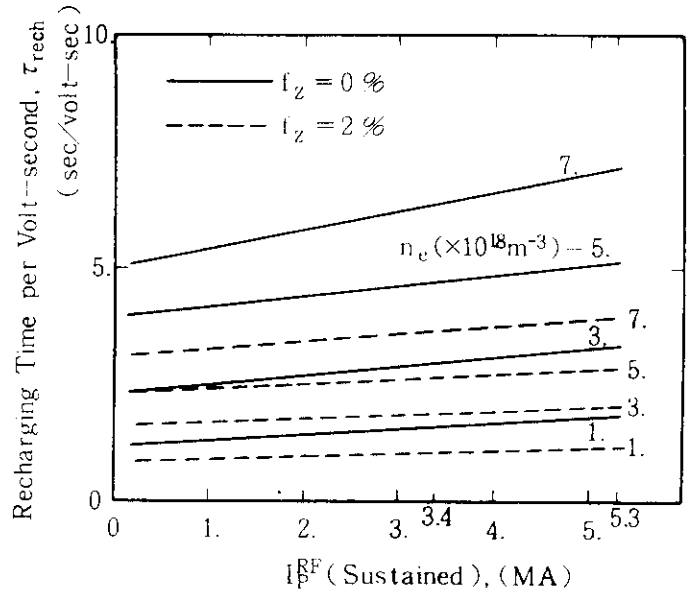

Fig. 8 Dependence of I_p^{RF} on recharging time for one volt-second concerning case A (Case B is 0.73 times long as Case A)

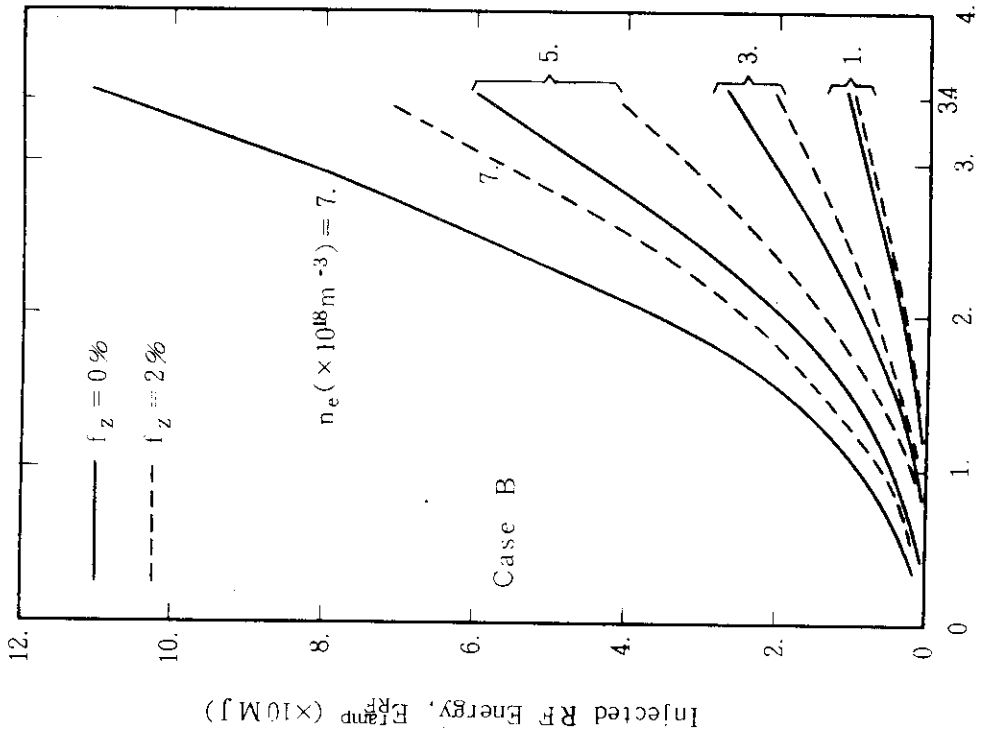

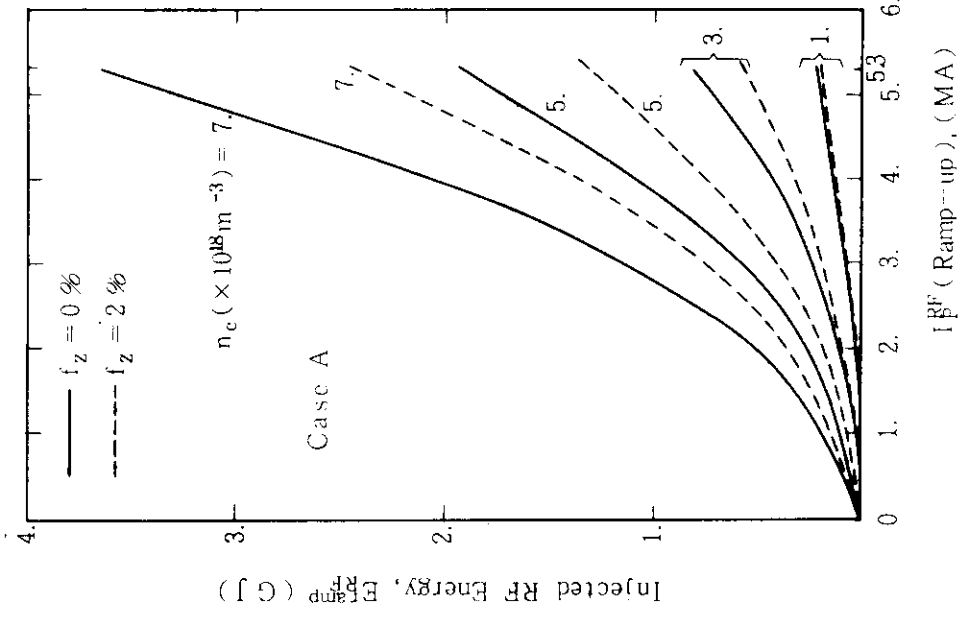

Fig. 9 Dependence of I_p^{RF} on injected RF energy

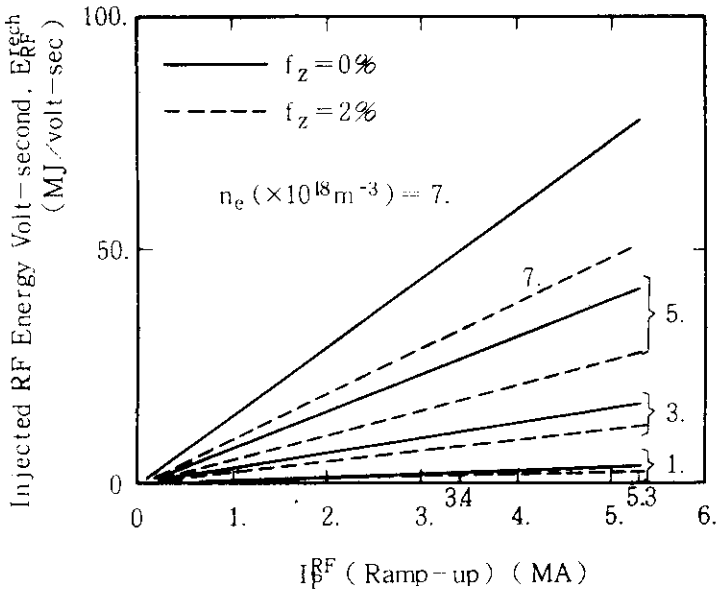

Fig.10 Dependence of I_p^{RF} on injected RF energy for one volt-second in recharging phase concerning case A (Case B is 1.04 times much as Case A)

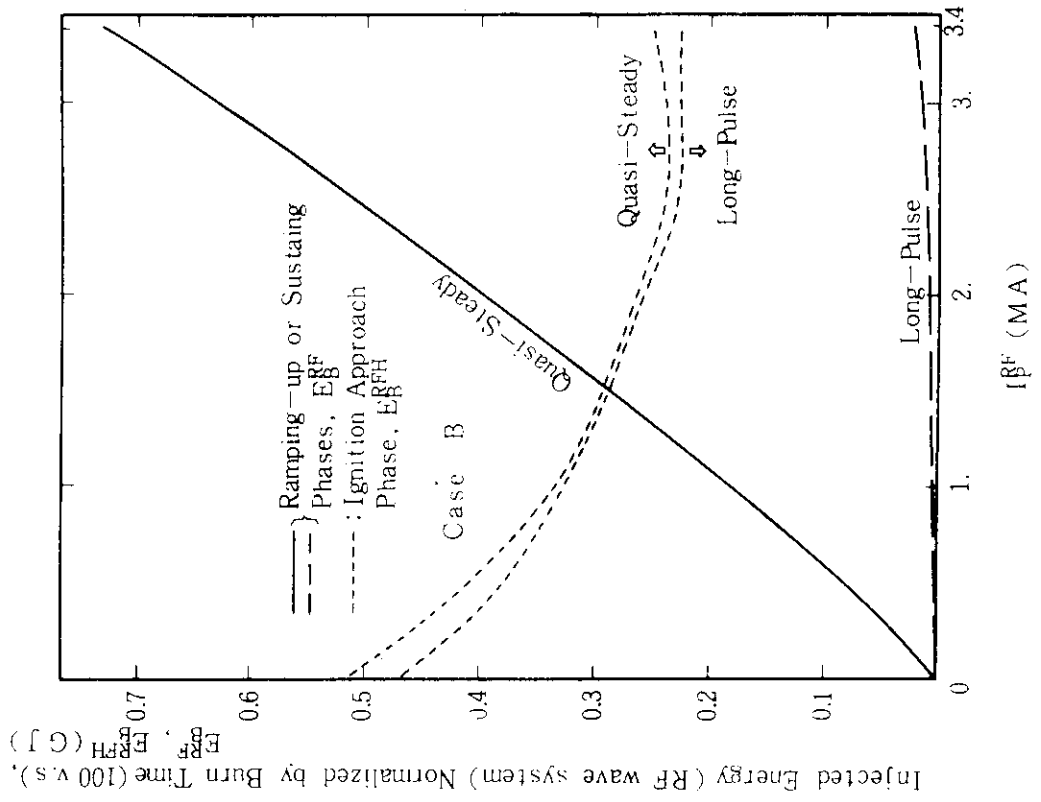

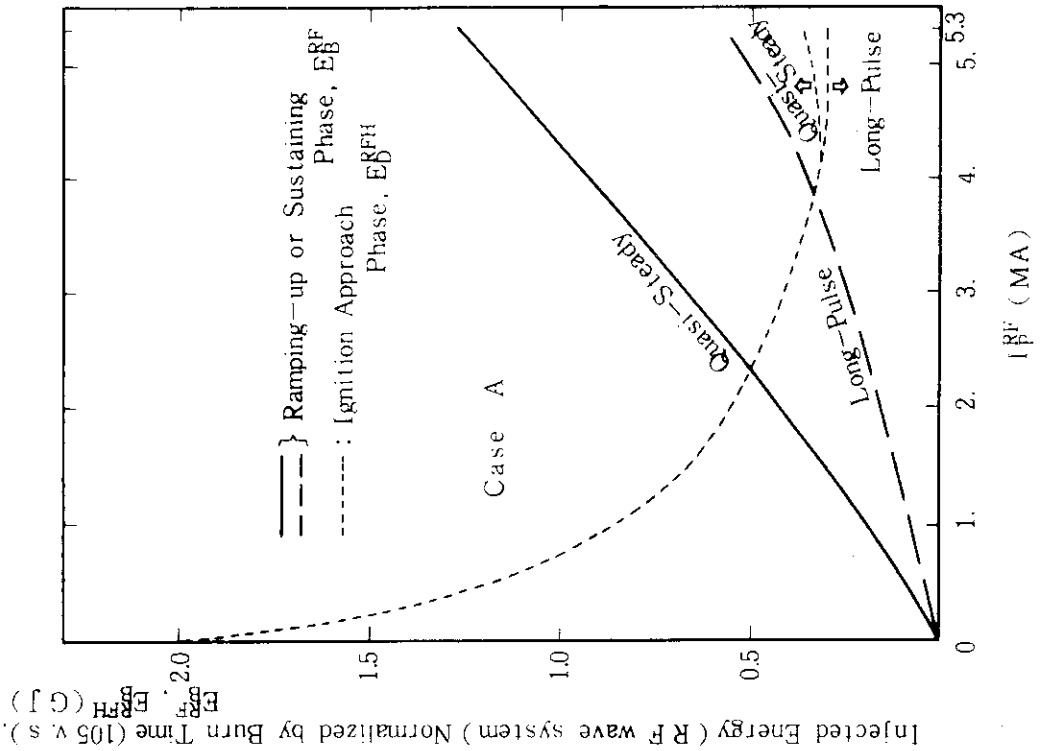

Fig.11 Dependence of I_p^{RF} on normarized RF energy

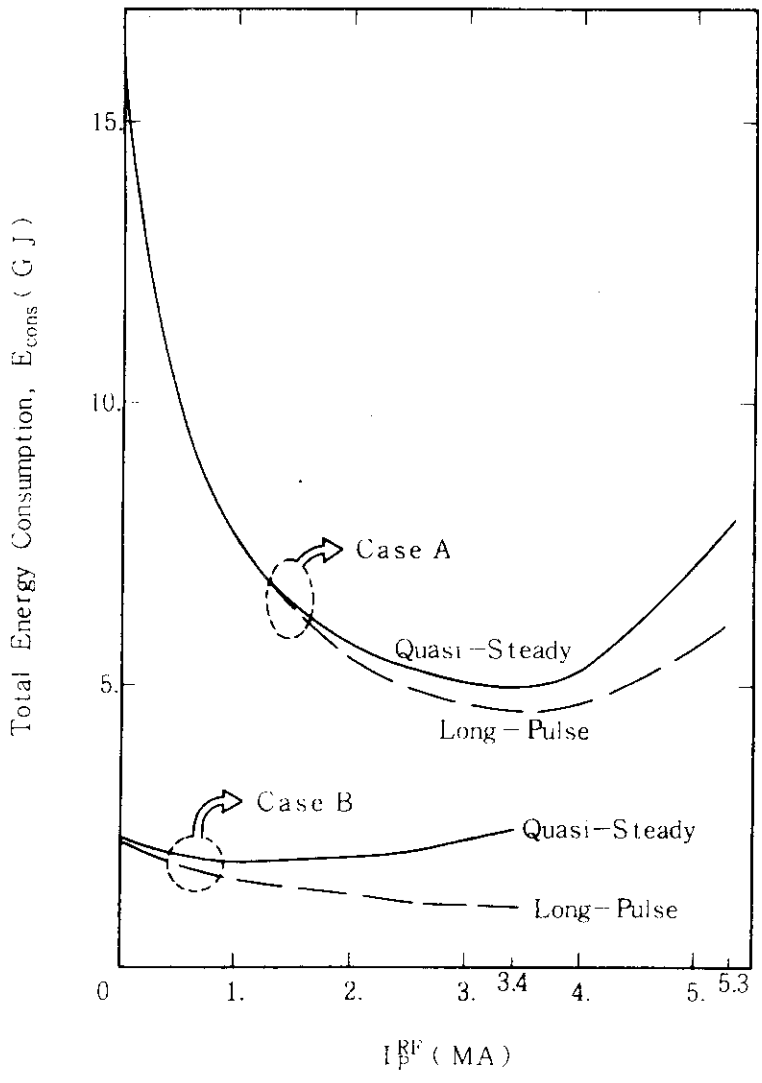

Fig.12 Dependence of I_p^{RF} on total energy consumption (Case A and Case B are normarized by 105 v.s and 100 v.s which are the maximum available volt-second for burn phase, respectively)

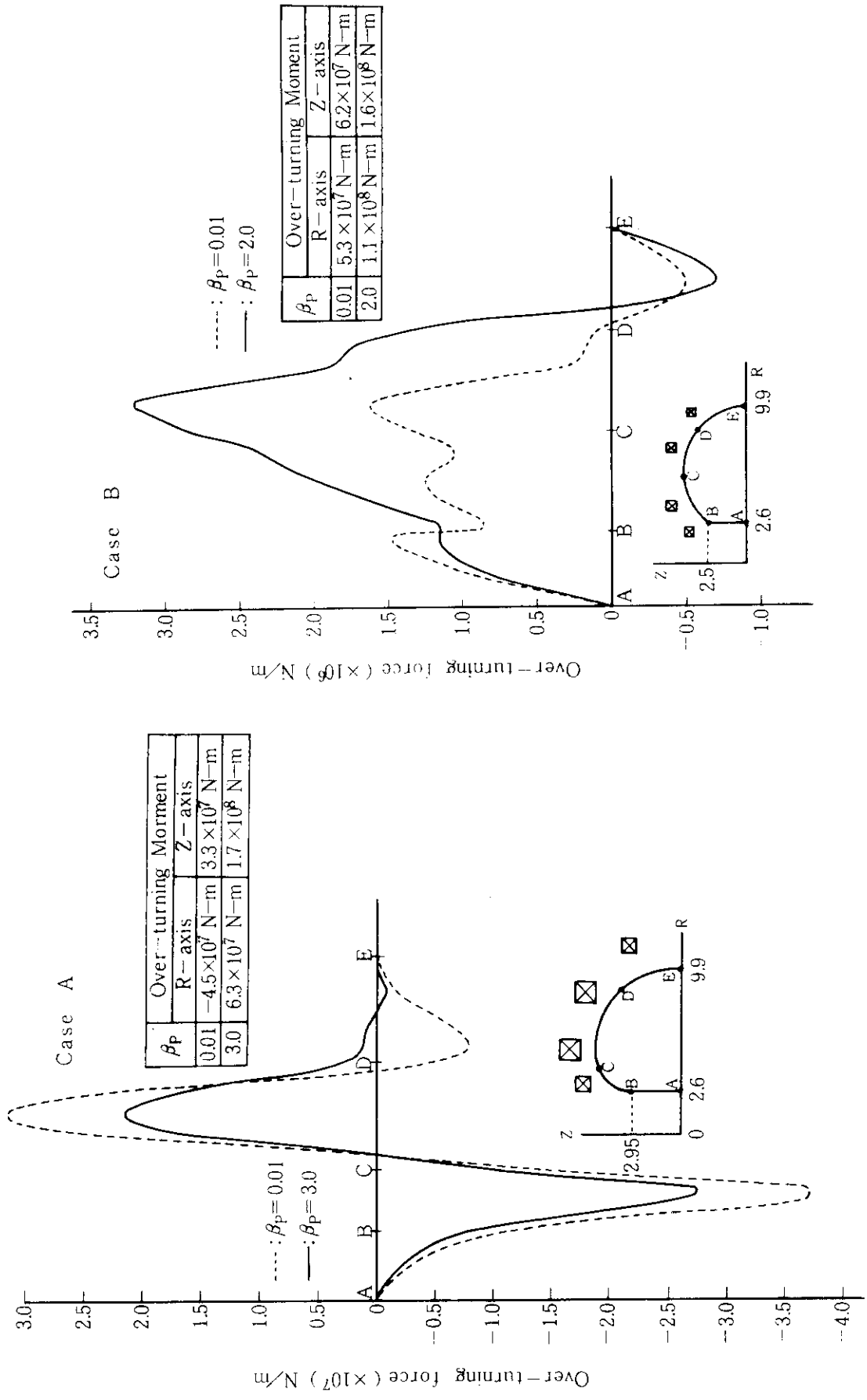

Fig.13 Overturning force distribution for low poloidal beta (0.01) and high poloidal beta (3.0)

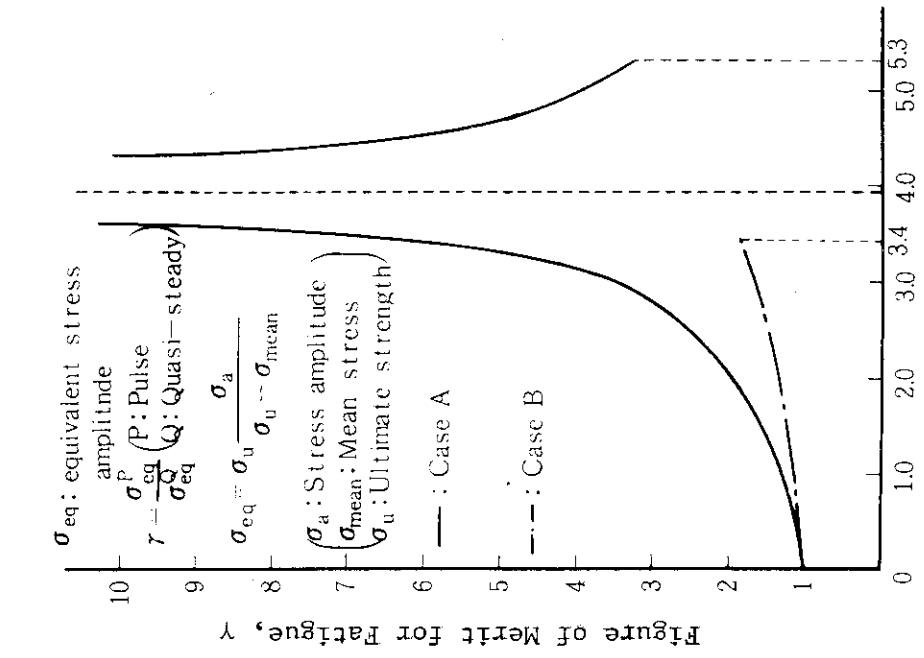

Fig.15 Dependence of I_p^{RF} on figure of merit for fatigue

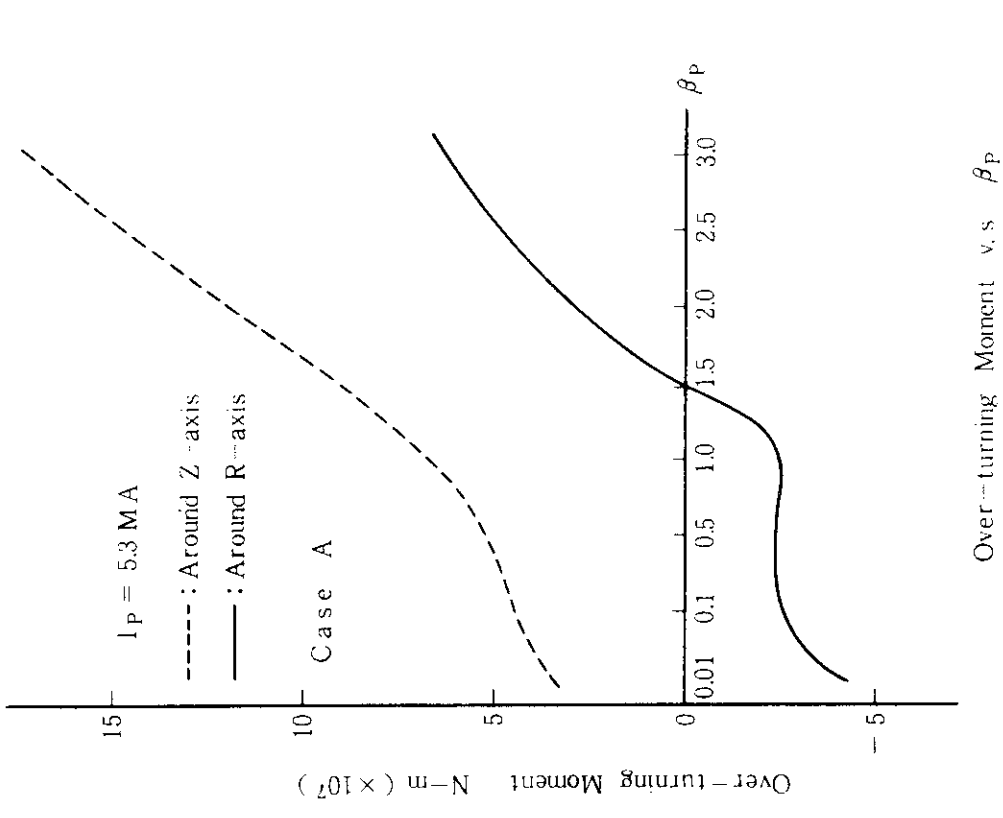

Fig.14 Dependence of poloidal beta on overturning moment as an integrated quantity (for Case A)

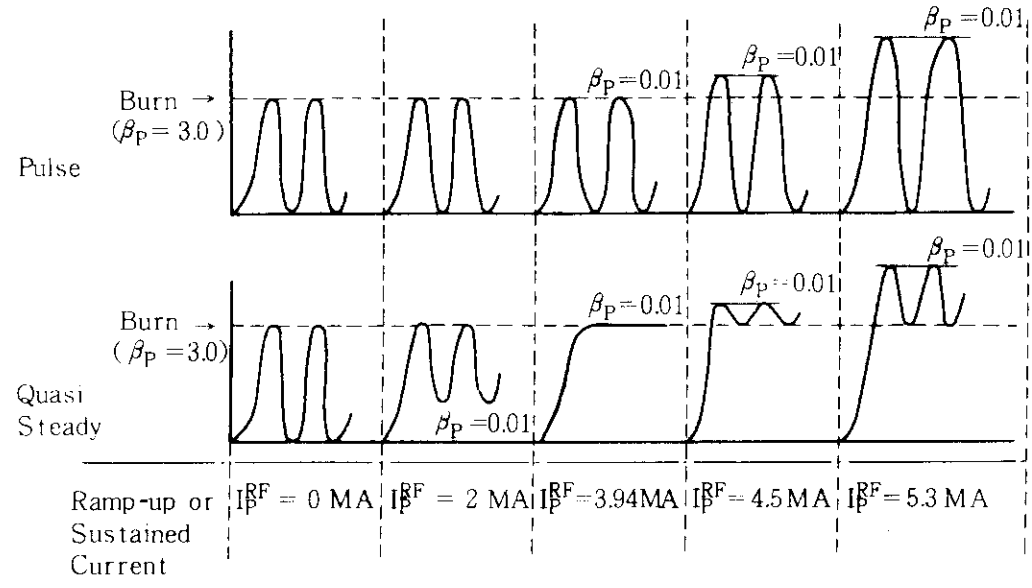

Case A

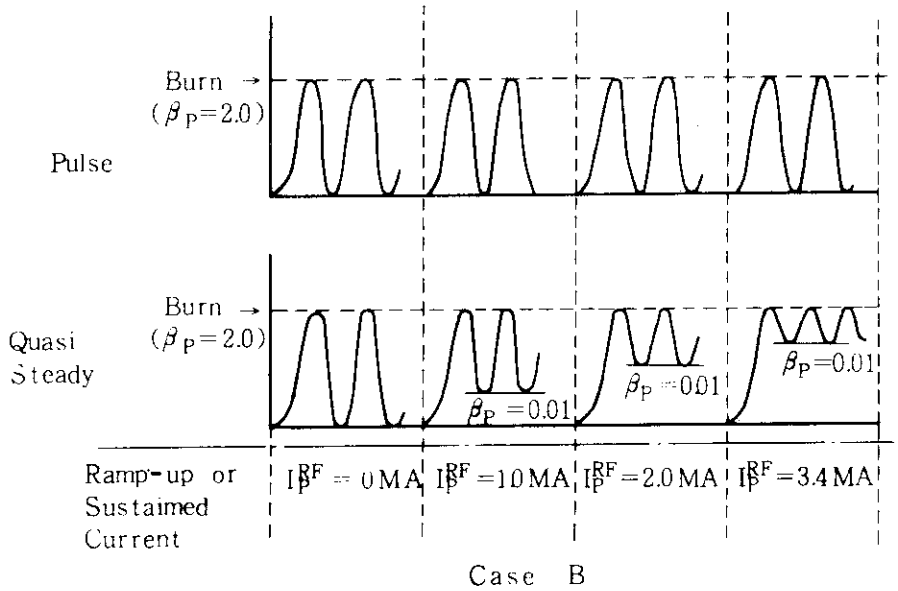

Case B

Fig.16 Scheme of stress amplitude for pulsed operation and for quasi-steady state operation

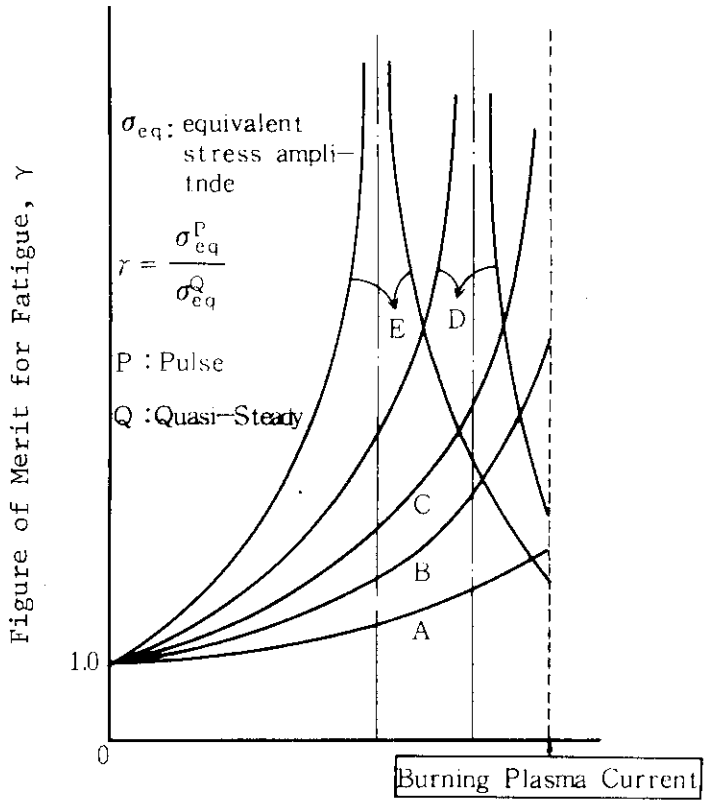

Fig.17 Dependence of I_p^{RF} on figure of merit for fatigue for several case of ellipticity (Ellipticity gradually increases from A to E)